Journal of Applied Polymer Science

Synthesis of Poly(oligo(ethylene glycol)methacrylate)-Functionalized Membranes for Thermally Controlled Drug Delivery

Francisco Teixeira Jr.,[1] Ana Maria Popa,[1] Sébastien Guimond,[2] Dirk Hegemann,[2] René M. Rossi[1]

[1]Laboratory for Protection and Physiology, Empa, Swiss Federal Laboratories for Materials Science and Technology, Lerchenfeldstrasse 5, St. Gallen, 9014, Switzerland

[1]Laboratory for Advanced Fibers, Empa, Swiss Federal Laboratories for Materials Science and Technology, Lerchenfeldstrasse 5, St. Gallen, 9014, Switzerland

Correspondence to: A. M. Popa (E-mail: ana-maria.buehlmann@empa.ch)

ABSTRACT: In this work a robust method for grafting thermoresponsive poly(oligo(ethylene glycol) methacrylates) (pOEGMA) macromolecules from polymeric porous membranes and silicon surfaces is presented. Hydrophilic track-etched polyester (PETE) membranes with submicrometer pore sizes and silicon dies were submitted to a plasma treatment, which successfully allowed the introduction of anchoring groups and further grafting of the initiator on the surface. The surface-initiated polymerization of OEGMA was carried out by atom transfer radical polymerization (ATRP), yielding dense polymer brushes. Moreover, the temperature-controlled transport of caffeine through the functionalized membranes was demonstrated and the influence of the pore morphology and immobilized polymer layer thickness on the permeation profile was investigated. © 2012 Wiley Periodicals, Inc. J. Appl. Polym. Sci. 129: 636–643, 2013

KEYWORDS: grafting; stimuli-sensitive polymers; membranes

Received 20 August 2012; accepted 14 October 2012; published online 19 November 2012
DOI: 10.1002/app.38730

INTRODUCTION

Stimuli-responsive polymers are macromolecular entities which undergo large conformational modifications upon specific condition changes in their physicochemical environment. Different trigger mechanisms have been investigated, among which light,[1] pH,[2,3] electric potential,[4] and temperature.[3–5] The latest is particularly relevant for physiological applications, as it can be tuned within a wide range, in a relatively noninvasive manner for living organisms. Micro- and nanoporous membranes functionalized with thermoresponsive polymers find applications in sensors,[6,7] filters,[8,9] textiles with enhanced comfort[10,11] or drug delivery systems.[12,13] Numerous reports describe the immobilization of poly-*N*-isopropylacrylamide (pNIPAAm), an amphiphilic polymer with a low critical solution temperature (LCST) in the physiological range (32°C)—on different substrates, such as colloidal films,[14] polymeric membranes,[9,15] and inorganic porous structures.[8,16,17] However, some empirical studies suggested that the acrylamide monomers and higher molecular mass polymers display important cytotoxicity,[18] which limits the application of these molecules in the biomedical domain. As such, more effort has been directed lately for the synthesis and characterization of homo- and copolymers with increased biocompatibility, such as poly(*N*-vinylcaprolactam)[19,20] and poly (oligo(ethylene glycol) methacrylate) (pOEGMA). An advantage of the pOEGMA systems is the possibility of controlling their LCST by simply modifying the composition of the OEGMA chain, as evidenced in the pioneering work of Lutz and Hoth.[21] By adding monomers with longer ethylene glycol side chains, the overall hydrophilicity of the macromolecules is increased and as a consequence, the LCST can be shifted to higher values.[21,22] Several works have also discussed the influence of environmental conditions[23] and the use of 1 different comonomers and end groups[24–27] on the LCST of the pOEGMAs. The versatility of these systems was exploited in the synthesis of thermoresponsive hydrogels with tunable optical properties[28] or matrices for drug delivery applications[29,30] Other investigations focused on the "grafting from" of pOEGMA chains onto suitable functionalized substrates, mostly gold,[31] silicon,[32] or polystyrene[33] with the aim of providing switchable wettability to the surfaces.[34,35] The grafting of pOEGMA from porous substrates has been only recently described[36] but their thermo-responsive character and hence potential for application in thermally-controlled drug delivery devices has not been thoroughly investigated.

In the present work we present the functionalization of track-etched polyester (PETE) porous membranes and silicon surfaces with different pOEGMA polymers by a surface-initiated Atom Transfer Radical Polymerization (si-ATRP) approach. The morphological

Additional Supporting Information may be found in the online version of this article.

modifications and the introduction of a stimuli-responsive character to the grafted membranes by the presence of these polymers on the surface are demonstrated. Moreover, the temperature-controlled permeation of caffeine—a model ingredient, relevant for both pharmaceutical and cosmetic applications—through the functionalized membranes is also shown.

EXPERIMENTAL

Materials

The 2-(2-methoxyethoxy)ethyl methacrylate (DEGMA, 95%, M_n = 188.22 g mol^{-1}), oligo(ethylene glycol) methacrylate (OEGMA, 98% M_n = 475 g mol^{-1}), 2,2-bipyridyl (Bipy), 2-bromoisobutyryl bromide (2-BIBB, 98%), methyl 2-bromopropionate (MBP, 98%), triethylamine (TEA, $\geq$ 99%), caffeine (anhydrous, $\geq$ 99.0%) and ethanol (anhydrous, $\geq$ 99.5%) were purchased from Aldrich, Switzerland and used as received. Copper bromide I (CuIBr, 99%, Aldrich) was washed with glacial acetic acid (Sigma–Aldrich) to remove any oxidized species, filtered and washed with ethanol and dried under vacuum. Dichloromethane was purchased from Fischer Scientific and used as received. B-doped [100]-oriented silicon wafers were acquired from Seltron, Korea. Cyclopore polyester track etched (PETE) membranes (0.2 μm pores, 25 mm diameter) were purchased from Whatman, USA.

Plasma Treatment

Plasma polymer coatings were deposited in a low pressure web coater consisting of a RF-driven (13.56 MHz) drum electrode (with a diameter of 59 cm and a length of 65 cm) enclosed in a larger cylindrical vacuum chamber. This pilot-scale plasma reactor has been described in more details elsewhere.[37] The membranes were fixed on the drum electrode and the latter was rotated during deposition to achieve a uniform coating on all substrates. Prior to the deposition, the samples were shortly cleaned and activated with Ar/O_2 plasma (10 Pa, 400 W, 160 sccm Ar, 40 sccm O_2 for 1 min) to ensure a good adhesion of the coating. Plasma polymerization was carried-out at a pressure of 10 Pa and with a plasma power input of 750 W, using gas flows of 250 sccm and 200 sccm for NH_3 and C_2H_4, respectively. A deposition time of 10 min was used for both the silicon wafers and each side of the PETE membranes.

Immobilization of the ATRP Initiator

A 2.4*M* TEA solution in DCM was prepared and transferred to a 50-mL round bottom flask containing a stirrer. A perforated stainless steel grid was inserted in the flask (to prevent contact with the stirrer and the membrane/wafer) and the membrane/wafer to be functionalized was immersed in the solution and placed onto it, being then transferred into an ice-water bath (0°C). A 1.6*M* solution of 2-BIBB in DCM was prepared and added drop-wise to the flask (volume ratio (v/v) for the TEA and 2-BIBB solutions: 1 : 1). The mixture was stirred and a bubbler was put on top of the flask. The reaction was left overnight, eventually reaching room temperature. The membranes/wafers were washed thoroughly with DCM ethanol and water respectively, and then placed in an ultrasonic bath, to remove any physically adsorbed residues or impurities from the reaction. They were then rinsed once again with ethanol and the membranes were dried at room temperature, while the Si wafers were dried under a nitrogen flow.

Grafting of Thermoresponsive Polymers

About 1 eq of CuIBr and 2 eq of Bipy were placed into 50-mL Schlenk flasks (dried at 130°C for 3 h immediately before the polymerization). A stirrer and a perforated stainless steel grid (to prevent contact with the stirrer and the membrane/wafer) were inserted in the flask and a single initiator-modified membrane/Si wafer was laid onto it. The system was vacuumed and successively backfilled with Ar three times. A solution containing 100 eq/200 eq of monomer and 1 eq of MBP in ethanol was purged with argon and transferred to the Schlenk flask with a syringe (previously purged with Ar). The reactor was put at 60°C for 3 h/6 h, respectively, for the polymerization to occur. After the reaction time was completed, the reactor was opened to air to deactivate the catalyst and terminate the reaction. The membrane/wafer was then removed from the Schlenk flask, washed thoroughly with ethanol, placed in an ultrasonic bath for 30 s and dried either at room temperature (membranes) or under a nitrogen flow (wafers). A sample of the polymer mixture was collected for gel permeation chromatography (GPC) analysis. The polymers were named according to the aimed LCST and degree of polymerization (DP).

Surface Characterization of the Functionalized Membranes

Scanning electron microscopy (SEM) imaging was conducted with a Hitachi S-4800 microscope. Because the surfaces are composed of nonconductive material, it was necessary to deposit a gold layer onto the samples to be able to analyze the surfaces. Given that in this case a large amount of gold could mask the measurement results by decreasing the size of the membrane pores, only a thin layer of gold ($\sim$ 2 nm) was deposited onto the membranes. The images were analyzed using the ImageJ software. X-ray photoelectron spectroscopy (XPS) analysis was performed using a PHI LS 5600 instrument with a standard Mg Kα X-ray source (nonmonochromatized). Spectra were acquired at a photoelectron take-off angle of 45°, and the binding energy scale was referenced to the C1s aliphatic carbon peak at 285 eV. The operating pressure of the XPS analysis chamber was 1×10^{-9} Torr. The spectra were processed using the CASA XPS software. Contact angles were measured with a Krüss G10 System, coupled to a Peltier element. The values reported are averaged from four measurements at different randomly chosen sites of the membranes. Ellipsometry measurements were performed on the grafted silicon wafers using an EP3 ellipsometer (Nanofilm). The wavelength was 532 nm and the angle of incidence was varied from 55° to 75° in 2° increments. The subsequent fitting of the data was performed with the EP3 software using a three layer model and the respective refractive indexes assumed for the different layers were 1.5 for the native SiO_2, 1.52 for the plasma polymer layer,[38] and 1.46 for the pOEGMA layer.[39]

Caffeine Permeation Measurements

Permeation measurements were performed in jacketed Franz cells (12 mL receptor chamber) with 100 m*M* caffeine solutions as donor and deionized water as receptor solution. 0.5 mL samples were collected every 30 min for 2.5 h to analyze the amount of caffeine that permeated through the membrane at different temperatures (20 and 40°C). The caffeine content analysis was performed using a Synergy Mx Spectrometer (Biotek). 250 μL of

Applied Polymer SCIENCE

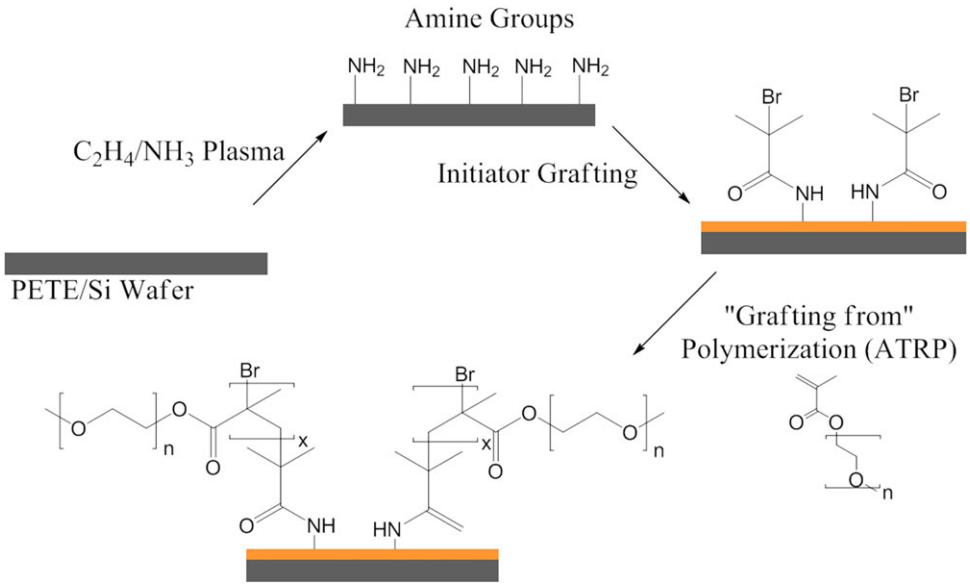

Figure 1. Schematic representation of the functionalization route for polymeric membranes and silicon surfaces, showing the plasma modification, the initiator immobilization and the "grafting from" of the polymers. [Color figure can be viewed in the online issue, which is available at wileyonlinelibrary.com.]

the samples were transferred to a 96-well plate and their respective optical measured at 300 nm.

RESULTS AND DISCUSSION

Plasma-assisted Functionalization of the Membranes and Grafting of the ATRP Initiator Layer

The synthetic route used in the preparation of thermoresponsive surfaces is summarized in Figure 1.

Porous PETE membranes were subject to plasma treatment to introduce nitrogen-containing functionalities (primary amino-groups) on their surface and allow the immobilization of the ATRP initiator.

Plasma polymerization is a form of plasma-enhanced chemical vapor deposition (PECVD), in which a gas discharge is used to activate gaseous monomers and initiate polymerization on a surface. It allows the deposition of thin, smooth, highly crosslinked, functional and well adherent polymer films.[40,41] By using a gas mixture of ethylene (C_2H_4) and ammonia (NH_3) in the discharge, crosslinked polymer thin films containing a relatively high concentration of primary amine groups can be deposited[42] at a rate of 2–3 nm min^{-1}. The density of primary amino-groups is dependent on the volumetric ratio of the feed-gases but also on the energy density during film growth.[43] The surface of a-C:H:N thin films deposited under similar plasma conditions was reported to contain about six to eight primary amines per 100 C atoms[42,43] as determined by X-ray photoelectron spectroscopy (XPS) after modification with 4-(trifuoromethyl)benzaldehyde (TFBA). Ellipsometry measurements on silicon wafers functionalized in parallel with the membranes confirmed a thickness of the anchoring layers of 29 ± 2 nm, which is well correlated with the value expected for the applied deposition time.

XPS measurements were performed after each step of the thermoresponsive membrane preparation, to evaluate whether the modifications were succesfull and determine the chemical composition of the membrane surfaces (Figure 2).

As such, in the analysis of the plasma treated surfaces the characteristic peak of the amino groups at 399.3 eV was observed, confirming the introduction of the anchoring groups. Furthermore, the relative atomic nitrogen concentration on the surface was found to be ~ 10% in respect to the other atoms (except hydrogen), in agreement with what is expected for this plasma functionalization methodology.[42]

Additionally, the changes in porosity and in pore morphology after the deposition of the amine functionalized plasma polymer layer on the PETE membranes were monitored by SEM (Figure 3).

As stated by the manufacturer, the pores of the pristine membranes were cylindrical (having been obtained by a track-etch

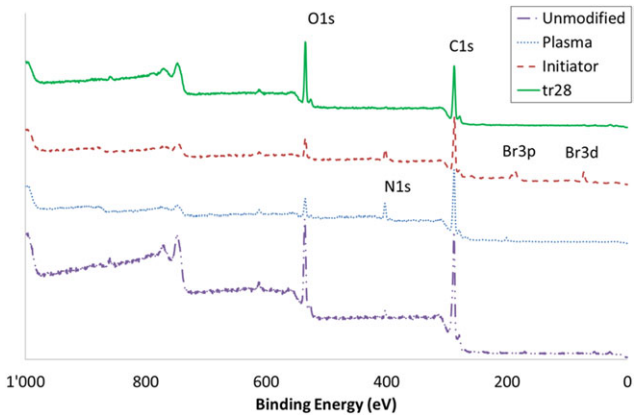

Figure 2. XPS spectra showing the evolution of the surface chemistry of a PETE membrane: unmodified (–¨–),C_2H_4/NH_3 plasma treatment (…), initiator grafting (– –) and grafting of the polymer tr28 (—).

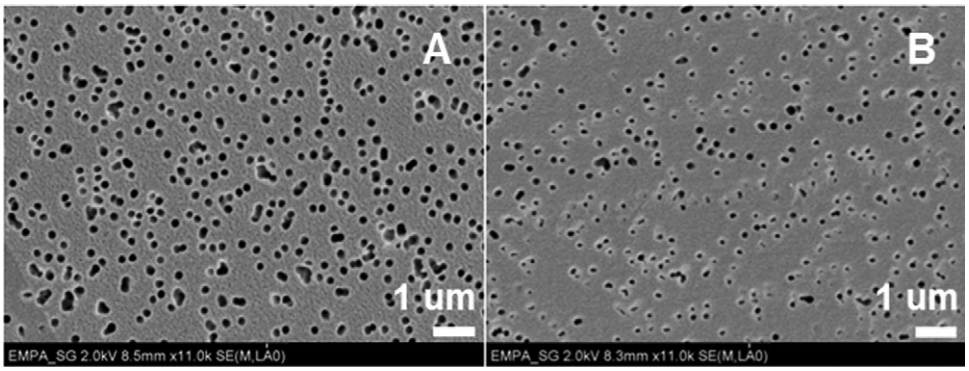

Figure 3. SEM micrographs of the PETE membranes: (A) unmodified and (B) after C_2H_4/NH_3 plasma treatment.

process) and their initial size was around 200 nm, with maximum diameters of 700 nm in the regions where pores overlapped. As expected, upon deposition of the plasma layer a difference in the membrane morphology was observed, with a clear reduction in membrane porosity. Both sides of the plasma-treated membranes were analyzed by SEM, showing a similar reduction in pore size. Because of the anisotropy of the plasma process[43] no active anchoring groups are formed inside the membrane pores.

After the plasma treatment, the initiator precursor, 2-bromoisobutyryl bromide (2-BIBB) was reacted in solution with the amine groups present on the surface of the membranes. The reaction between acyl halide and amines is quantitative, due to the high electrophilicity of the acyl groups. Upon attachment of 2-BIBB the peak corresponding to nitrogen atoms in the XPS spectrum was shifted to 400.2 eV, which confirmed the formation of C—N bonds. In addition, the characteristic peaks for bromine (Br3p = 183.4 eV and Br3d = 69.8 eV) were observed, indicating that the initiator was covalently linked to the surface of the membrane.

Grafting of the Thermoresponsive Polymers by ATRP

The grafting of the thermoresponsive polymers was performed in *triplica* via ATRP using either DEGMA or a mixture of DEGMA/OEGMA (95 : 5) as monomers (Table I). These monomer feeds were chosen because the resulting polymers would have a LCST in the physiological range,[44] at 28 and 33°C, respectively.[20] A first observation concerning the evolution of the surface chemistry after grafting is that the peaks corresponding to N1s, Br3p, and Br3d electrons are not detectable anymore in the XPS spectra (Figure 2). This is mainly an indication that a thick polymer layer was grafted on the surface; it is also possible however that not all initiator groups reacted to yield a polymer chain. Additionally, an increase in the relative intensity of the O1s peak as compared to the C1s peak was observed. The relative concentrations of oxygen and carbon atoms are in good agreement with theoretical values (see Supporting Information for a detailed deconvolution of the C1s peak of tr28(100)PETE membrane, Figure S2).

SEM imaging allowed the analysis of the polymeric layer morphology (Figure 4). The pores of the PETE membrane grafted with tr28(100) [Figure 4(A)] are partially covered by the polymer layer, and the larger coalesced pores appear polymer free. Similar morphology changes can be observed for the tr33(100)PETE [Figure 4(C)]. The polymer layer has in both cases a grain-like structure, which may be indicative of a lower grafting density. As expected, in the case of the tr28(200)PETE [Figure 4(B)] most of the pores appear covered by a homogeneous polymer layer, which suggests the formation of a thick polymer brush for this particular polymerization degree.

SEM imaging was performed on the top and bottom surfaces of the membranes after grafting of the thermoresponsive polymers, revealing consistent morphological characteristics on both sides. Polymer deposition did not occur inside the pores, thus confirming the anisotropic nature of the plasma process used (cross-sectional images are presented in the Supporting Information Figure S1).

To infer the actual grafting density of the polymeric layers, ellipsometry measurements were performed on flat silicon wafers which were functionalized with tr28(100), tr28(200), and tr33(100) respectively (Table II). The use of silicon wafers as substrate for the analysis of polymer surface-grafted polymers is widely described in literature[44–47] and its extrapolation to thin porous membranes was recently reported as well.[48,49]

The pOEGMA thicknesses obtained by ellipsometry, the respective M_n, the grafting density, interdistance chains and stretching parameters are summarized in Table II. The grafting density (Σ) is calculated according to eq. (1):

$$\Sigma = \frac{h\rho N_A \cdot 10^{-23}}{M_n} \quad (1)$$

where h is the thickness as determined by ellipsometry, ρ is the density of the polymer brush, assumed in this case to be 1 g cm^{-3},[50] N_A is Avogadro's number and M_n is the molecular weight of the polymeric chains.

Table I. Theoretical Composition and Expected LCST[21] of the Thermoresponsive Polymers Grafted onto the Membranes/Wafers

Name	DEGMA : OEGMA ratio	DP (theoretical)	LCST (°C)
tr28(100)	100 : 0	100	28
tr28(200)	100 : 0	200	28
tr33(100)	95 : 5	100	33
tr33(200)	95 : 5	200	33

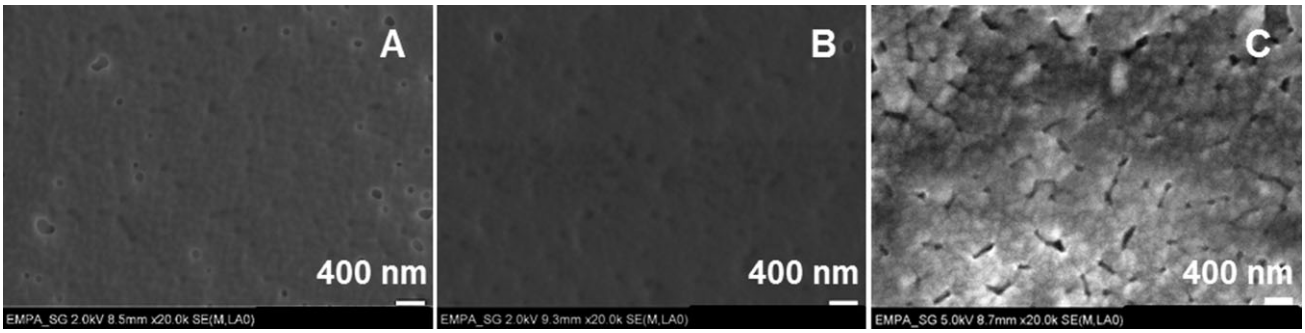

Figure 4. SEM micrographs of the PETE membranes after polymer grafting with (A) tr28(100), (B) tr28(200), and (C) tr33(100).

The distance between two adjacent chains (D) is calculated with the formula:

$$D = \sqrt{\frac{4}{\pi\Sigma}} \tag{2}$$

The Flory radius of the poly(oligo(ethylene glycol) methacrylate) chains was approximated with the formula:

$$Rf = aN^{3/5} \tag{3}$$

where a is the length of the statistic segment and has a value of 0.3 nm for flexible polymers and N is the polymerization degree.

In all cases the grafting density is relatively high and the interchain distance much lower than the Flory radius of the polymers. The ratio between the interchain distance (D) and the double of the Flory radius (R_f) can be interpreted in a qualitative manner as a measure of the stretching degree. In the case of the oligo (ethylene glycol) methacrylate copolymers this value is higher than 0.1, which suggests that the macromolecular chains on the surface adopt a mushroom conformation.[17] Additionally, the tr28(200) brush appears to have the highest grafting density and the highest stretching degree, and this observation is well correlated with the smoother morphology of the corresponding polymer films, observed by SEM. Finally, the calculated grafting density appears to be quite high for the tr33(100) polymer, but this value is most likely overestimated, since the Flory radius approximation does not take into account the larger excluded volume of the OEGMA monomers (as compared to DEGMA).

Thermoresponsive Character of the Functionalized Membranes

The thermoresponsive character of the functionalized membranes was first probed in a qualitative manner by water contact angle (WCA) measurements below and above their transition temperature, at 25 and 40°C, respectively. It is expected that the LCST of grafted polymers does not differ substantially from the one of polymers previously synthesized in solution.[17] In brief, these measurements confirmed a remarkable change in the surface hydrophilicity upon polymer grafting (Supporting Information Table SI). Upon heating the substrate functionalized with tr28(100) above the transition temperature of the polymer (28°C), the contact angle increased from below 5° to 44° ± 4° on the PETE membranes. This increase in the surface hydrophobicity is expected, as upon the grafted polymer collapse above the LCST the more hydrophobic moieties are exposed to the surface.

Moreover, the influences of both the pore morphology and the polymer brush grafting density on the thermoresponsive gating properties of the membranes were assessed by caffeine permeation assays below and above the LCST.

Caffeine was chosen as a model compound due to its small size, water solubility, and straightforward detection via UV–vis spectrometry. Given that PEG chains are known for their antifouling properties, being used, for instance, as protein repellent coatings[51,52] low adsorption of the caffeine on the polymer-modified membranes is expected.

The results of the permeation assays through the PETE membranes showed that the permeability of caffeine across all the membranes, regardless of their surface chemistry or pore dimensions, was higher at 40°C than at 20°C (Figure 5). Even for the blank PETE membranes, the increase in permeation upon increase in temperature was as high as 29%. This effect is to be expected, since an increase in temperature also increases the relative mobility of the molecules, and consequently their diffusion rate.

Table II. Overview of the Respective Ellipsometric Thickness of the Three Polymeric Layers Grafted on the Si Wafers, the Corresponding Theoretical Grafting Densities, Characteristic Distance Between Two Adjacent Chains and Respective Stretching Degree ($D/2R_f$)

Sample	Thickness (nm)	$M_{n,th}$[a] (kDa/mol)	Σ_{th} (chains/nm^2)	D_{th} (nm)	$R_{f,th}$ (nm)	$D/2R_f$
tr28(100)Si	41 ± 1	18.8	0.22	2.39	7.7	0.16
tr28(200)Si	64 ± 3	37.6	0.17	2.70	11.6	0.12
tr33(100)Si	58 ± 2	20.2	0.29	2.09	7.7	0.14

[a]As predicted from the aimed polymerization degree.

The diffusional fluxes of caffeine across the PETE membranes were used to characterize their permeability.[53,54] The permeation through the polymer-grafted PETE membranes is considerably lower than what was observed for the unmodified ones at both temperatures, due to the molecular crowding caused by the polymer chains around the pores. This effect is even clearer for the tr28(200) polymer, which causes a dramatic reduction in the permeability of the PETE membranes. However, the proportional increase in caffeine flux resulting from the temperature change to 40°C (above the LCST of the polymers) is much higher than what was observed for the blank membranes, namely 40–50% for tr28(100)PETE and around 1000% for tr28(200)PETE (Table III). These increases are a consequence of the collapse of the grafted polymer brush and subsequent opening of the pores, while the more prominent change in permeation observed for TR28(200)PETE is due to the length of the grafted polymer chains, causing a higher molecular crowding around the pores.[55]

The results of the permeation assays for the tr33(100)PETE membranes (Table III) show that their permeability below and above the LCST is lower than what was observed for the tr28(100)PETE. This is to be expected, since the excluded volume of the longer oligo(ethylene glycol) methacrylate chains is larger, leading to a greater molecular crowding when compared to the relatively short side chains of the 2-(2-methoxyethoxy)ethyl methacrylate. Moreover, the differences in permeation through the tr28(100)PETE and tr33(100)PETE membranes are well explained by the differences observed in the grafting densities and the morphology of the respective substrates.

It is important to note that the caffeine permeation through the PETE membranes occurs according to two different diffusion regimes. In the first 60 min, the process follows Fick's first law of diffusion, since the concentration gradient between the two chambers of the Franz's cell is high and the concentration change in the receptor chamber can be neglected. After that, however, the concentration gradient decreases and the concentration changes become significant as the system draws closer to equilibrium, leading to a regime better described by Fick's second law.

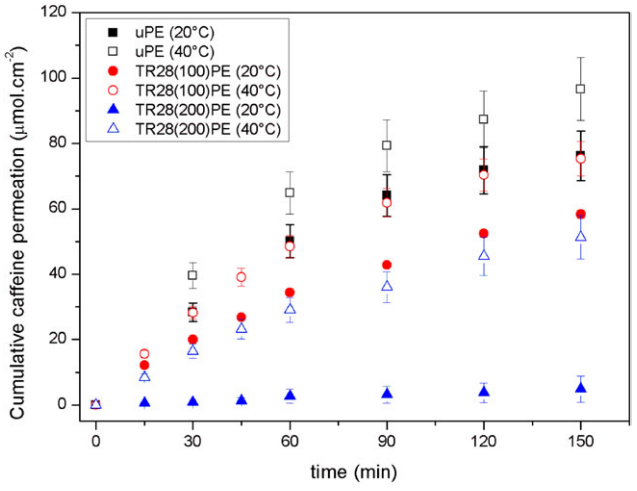

Figure 5. Cumulative amount of caffeine permeated through unmodified (uPETE) and modified PETE membranes at 20 and 40°C in a Franz cell experiment, as a function of time (as detected by UV–vis spectroscopy analysis of samples collected periodically). [Color figure can be viewed in the online issue, which is available at wileyonlinelibrary.com.]

Table III. Diffusion Fluxes of Caffeine for the PETE Membranes at Different Temperatures

	Caffeine flux (µmol cm^{-2} h^{-1})	
Membrane type	20°C	40°C
Unmodified PETE	50.1 ± 2.2	64.9 ± 4.7
TR28(100)PETE	33.4 ± 2.3	48.2 ± 2.8
TR28(200)PETE	2.5 ± 0.5	29.2 ± 1.3
TR33(100)PETE	20.0 ± 0.8	35.7 ± 0.8

Several works describe how the grafting of thermoresponsive pNIPAAM to polymeric membranes affect their barrier properties in permeation assays with a number of compounds, such as dextrans[56,57] tryptophan,[58] and vitamin B_{12}.[59] At low and intermediate polymer grafting densities, the permeation of small molecules is hindered by the extended polymeric chains. Once the temperature is raised above the LCST the grafted chains collapse, resulting in an increase of the pore area and consequently in permeability. The extent of this change is dependent both on the density of polymer grafted into the pores, as well as on the pore morphology.[14,56,57,60] Our observations on the pDEGMA and pDEGMA-co-OEGMA grafted membranes are in good agreement with these previously reported results.

CONCLUSIONS

A straightforward approach for producing thermoresponsive polymeric membranes, combining the plasma-assisted functionalization and subsequent "grafting from" of poly(oligo (ethylene glycol) methacrylate) copolymers was shown. The chemical characterization of the surfaces by XPS demonstrated the successful surface-initiated ATRP of the pOEGMAs. Moreover, the calculation of the polymer grafting density on the surface as determined from the ellipsometric thickness of the immobilized polymer layers indicated the formation of well-defined brushes. Finally, the polymeric chains tethered to the membranes clearly introduced a stimuli-responsive characteristic to the surfaces. The control over the amount of caffeine that permeates though the membranes is based on the conformational change of the polymeric chains upon a temperature change above the LCST, and was shown to be dependent on the length and excluded volume of the polymer brush. More specifically, an important increase (~ 10 fold) in the caffeine flux was observed for the sample functionalized with thicker polymer layers (tr28(200)PETE)).

Besides the application explored in this work, namely the temperature-controlled delivery of active ingredients, the obtained membranes have potential applications in sensing and filtration applications where a sharp temperature response and low surface fouling is needed.

ACKNOWLEDGMENTS

The authors thank Barbara Hanselmann for her assistance in performing the plasma treatment of the membranes used in this work.

REFERENCES

1. Narayan, K. S.; Kumar, N., *Appl. Phys. Lett.* **2001**, *79*, 1891.
2. Dai, S.; Ravi, P.; Tam, K. C. *Soft Matter* **2008**, *4*, 435.
3. Filipcsei, G.; Feher, J.; Zrinyi, M. *J. Mol. Struct.* **2000**, *554*, 109.
4. Yuk, S. H.; Cho, S. H.; Lee, S. H. *Macromolecules* **1997**, *30*, 6856.
5. Okano, T. *Adv. Polym. Sci.* **1993**, *110*, 179.
6. Iwai, K.; Matsumura, Y.; Uchiyama, S.; Prasanna, A. *J. Mater. Chem.* **2005**, *15*, 2796.
7. Ryu, S.; Yoo, I.; Song, S.; Yoon, B.; Kim, J. M. *J. Am. Chem. Soc.* **2009**, *131*, 3800.
8. Rao, G. V. R.; Krug, M. E.; Balamurugan, S.; Xu, H.; Xu, Q.; López, G. P. *Chem. Mater.* **2002**, *14*, 5075.
9. Liu, Y. L.; Han, C. C.; Wei, T. C.; Chang, Y. *J. Polym. Sci. Polym. Chem.* **2010**, *48*, 2076.
10. Crespy, D.; Rossi, R. M. *Polym. Int.* **2007**, *56*, 1461.
11. Kaursoin, J.; Agrawal, A. K. *J. Appl. Polym. Sci.* **2007**, *103*, 2172.
12. Meng, F.; Zhong, Z.; Feijen, J. *Biomacromolecules* **2009**, *10*, 197.
13. Chung, J. E.; Yokoyama, M.; Yamato, M.; Aoyagi, T.; Sakurai, Y., Okano, T. *J. Control. Release* **1999**, *62*, 115.
14. Schepelina, O.; Zharov, I. *Langmuir* **2007**, *23*, 12704.
15. Yu, J. Z.; Zhu, L. P.; Zhu, B. K.; Xu, Y. Y. *J. Membr. Sci.* **2011**, *366*, 176.
16. Liang, L.; Liu, J.; Gong, X. *Langmuir* **2000**, *16*, 9895.
17. Popa, A. M.; Angeloni, S.; Buergi, T.; Hubbell, J. A.; Heinzelmann, H.; Pugin, R. *Langmuir* **2010**, *26*, 15356.
18. Vihola, H.; Laukkanen, A.; Valtola, L.; Tenhu, H.; Hirvonen, J. *Biomaterials* **2005**, *26*, 3055.
19. Crespy, D.; Golosova, A.; Makhaeva, E.; Khokhlov, A. R.; Fortunato, G.; Rossi, R. M. *Polym. Int.* **2009**, *58*, 1326.
20. Crespy, D.; Zuber, S.; Turshatov, A.; Landfester, K.; Popa, A. M. *J. Polym. Sci. A Polym. Chem.* **2012**, *50*, 1043.
21. Lutz, J. F.; Hoth, A. *Macromolecules* **2006**, *39*, 893.
22. Yamamoto, S. I.; Pietrasik, J.; Matyjaszewski, K. *J. Polym. Sci. A Polym. Chem.* **2008**, *46*, 194.
23. Magnusson, J. P.; Khan, A.; Pasparakis, G.; Saeed, A. O.; Wang, W.; Alexander, C. *J. Am. Chem. Soc.* **2008**, *130*, 10852.
24. Jones, J. A.; Novo, N.; Flagler, K.; Pagnucco, C. D.; Carew, S.; Cheong, C.; Kong, X. Z.; Burke, N. A. D.; Stöver, H. D. H. *J. Polym. Sci. A Polym. Chem.* **2005**, *43*, 6095.
25. Ishizone, T.; Seki, A.; Hagiwara, M.; Han, S. *Macromolecules* **2008**, *41*, 2963.
26. Becer, C. R.; Hahn, S.; Fijten, M. W. M.; Thijs, H. M. L.; Hoogenboom, R.; Schubert, U. S. *J. Polym. Sci. A Polym. Chem.* **2008**, *46*, 7138.
27. Roth, P. J.; Jochum, F. D.; Forst, F. R.; Zentel, R.; Theato, P. *Macromolecules* **2010**, *43*, 4638.
28. Kubota, N.; Tatsumoto, N.; Sano, T.; Matsukawa, Y. *J. Appl. Polym. Sci.* **2001**, *80*, 798.
29. Liu, S.; Armes, S. P. *J. Am. Chem. Soc.* **2001**, *123*, 9910.
30. Ooyaa, T.; Leeb, J.; Park, K. *J. Control. Release.* **2003**, *93*, 121.
31. Hucknall, A.; Rangarajan, S.; Chilkoti, A. *Adv. Mater.* **2009**, *21*, 2441.
32. Gao, X.; Kucerka, N.; Nieh, M. P.; Katsaras, J.; Zhu, S.; Brash, J. L.; Sheardown, H. *Langmuir* **2009**, *25*, 10271.
33. Cheng, G.; Melnichenko, Y. B.; Wignall, G. D.; Hua, F.; Hong, K.; Mays, J. W. *Macromolecules* **2008**, *41*, 9831.
34. Xin, B.; Hao, J. *Chem. Soc. Rev.* **2010**, *39*, 769.
35. Dey, S.; Kellam, B.; Alexander, M. R.; Alexander, C.; Rose, F. R. A. *J. Mater. Chem.* **2011**, *21*, 6883.
36. Meng, J. Q.; Chen, C. L.; Huang, L. P.; Du, Q. Y.; Zhang, Y. F. *Appl. Surf. Sci.* **2011**, *257*, 6282.
37. Hossain, M. M.; Müssig, J.; Herrmann, A. S.; Hegemann, D. *J. Appl. Polym. Sci.* **2009**, *111*, 2545.
38. Birch, J. R.; Simonis, G. J.; Afsar, M. N.; Clarke, R. N.; Dutta, J. M.; Frost, H. M.; Gerbaux, X.; Hadni, A.; Hall, W. F., Heidinger, R.; Ho, W. W.; Jones, C. R.; Koniger, F.; Moore, R. L.; Matsuo, H.; Nakano, T.; Richter, W.; Sakai, K.; Stead, M. R.; Stumper, U.; Vigil, R. S.; Wells, T. B. *IEEE Trans Microwave Theory* **1994**, *42*, 956.
39. Lee, B. S.; Chi, Y. S.; Lee, K. B.; Kim, Y. G.; Choi, I. S. *Biomacromolecules* **2007**, *8*, 3922.
40. Siow, K. S.; Britcher, L.; Kumar, S.; Griesser, H. J. *Plasma Process. Polym.* **2006**, *3*, 392.
41. Hegemann, D. *Indian J. Fibre Text.* **2006**, *31*, 99.
42. Truica-Marasescu, F.; Wertheimer, M. R. *Plasma Process. Polym.* **2008**, *5*, 44.
43. Guimond, S.; Schütz, U.; Hanselmann, B.; Körner, E.; Hegemann, D. *Surf. Coat. Technol.* **2011**, *205*, S447.
44. Plasencia, I.; Norlen, L.; Bagatolli, L. A. *Biophys. J.* **2007**, *93*, 3142.
45. Feng, W.; Brash, J.; Zhu, S. *J. Polym. Sci. A Polym. Chem.* **2004**, *42*, 2931.
46. Liu, Y.; Klep, V.; Zdyrko, B.; Luzinov, I. *Langmuir* **2005**, *21*, 11806.
47. Wu, T.; Gong, P.; Szleifer, I.; Vlcek, P.; Subr, V.; Genzer, J. *Macromolecules* **2007**, *40*, 8756.
48. Tsujii, Y.; Ohno, K.; Yamamoto, S.; Goto, A.; Fukuda, T. *Adv. Polym. Sci.* **2006**, *197*, 1.
49. Singh, N.; Chen, Z.; Tomer, N.; Wickramasinghe, S. R.; Soice, N.; Husson, S. M. *J. Membr. Sci.* **2008**, *311*, 225.
50. Brass, D. A.; Shull, K. R. *J. Appl. Phys.* **2008**, *103*, 073517.

51. Langer, R.; Tirrell, D. A. *Nature* **2004**, *428*, 487.
52. Wischerhoff, E.; Uhlig, K.; Lankenau, A.; Börner, H. G.; Laschewsky, A.; Duschl, C.; Lutz, J. F. *Angew. Chem. Int. Ed.* **2008**, *47*, 5666.
53. Park, Y. S.; Ito, Y.; Imanishi, Y. *Langmuir* **1998**, *14*, 910.
54. Shim, J. K.; Na, H. S.; Lee, Y. M.; Huh, H.; Nho, Y. C. *J. Membr. Sci.* **2001**, *190*, 215.
55. Ying, L.; Kang, E. T.; Neoh, K. G.; Kato, K.; Iwata, H. *J. Membr. Sci.* **2004**, *243*, 253.
56. Lokuge, I.; Wang, X.; Bohn, P. W. *Langmuir* **2007**, *23*, 305.
57. Hesampour, M.; Huuhilo, T.; Makinen, K.; Manttari, M.; Nystrom, M. *J. Membr. Sci.* **2008**, *310*, 85.
58. Chu, L. Y.; Niitsuma, T.; Yamaguchi, T.; Nakao, S. I. *Aiche J.* **2003**, *49*, 896.
59. Wan, L. S.; Yang, Y. F.; Tian, J.; Hu, M. X.; Hu, Z. K. *J. Membr. Sci.* **2009**, *327*, 174.
60. Alem, H.; Duwez, A. S.; Lussis, P.; Lipnik, P.; Jones, A. M.; Champagne, S. D. *J. Membr. Sci.* **2008**, *308*, 75.